Optimal response of conical tool semi angle in ductile metal sheets indentation and its governing mechanics

Malik M. Nazeer†, M. Afzal Khan‡ and A-ul Haq‡

Dr. A. Q. Khan Research Laboratories, P.O. Box 502, Rawalpindi, Pakistan

Abstract. The nonlinear dependence aspect of various conical tool indentation parameters leading to an optimum tool semi angle value for easiest perforation is plotted and discussed explicitly in this work with the conclusion that tool angle has an optimum response towards most of the indentation parameters. Around this optimum angle, the aluminium sheets showed minimum fracture toughness as well as minimum work input to overcome the offered resistance. At the end, the mechanism leading to this phenomenon is presented with the conclusion that plastic flow dominates as the dimple semi cone angle reaches 35 and both pre and post plastic flow perforations lead the tool semi cone angle value towards this dimple cone semi angle of plastic flow initiation for its optimum performance. It is also concluded that specimen material failure is solely under tensile hoop stress and hence results into radial cracks initiation and propagation.

Key words: hoop stress; pre & post plastic flow juncture; perforations; crack propagation; perforation mechanics; premature death of cracks.

1. Introduction

Indentation and perforation of ductile metal sheet with conical tool (Fig. 1) is composed of elasto-plastic bending, stretching, plastic flow, perforation, cracks initiation and propagation ultimately resulting into material fracture with number of petals formation (Fig. 2). This perforation and petal formation is the result of complicated modes of deformations depending on the metal properties, tool angle, sheet thickness; indentation speed and size of the sample holding die as elaborated by Khan *et al.* (1995). The process of conical tool indentation was studied and mathematically analyzed by Khan (1996) and Nazeer *et al.* (2000). With the help of this analysis and computer code developed by Khan (1996) and Nazeer *et al.* (2000), the sheet thickness response was presented by Nazeer *et al.* (1997), while the response of a few other parameters versus tool displacement was presented and discussed by Nazeer* *et al.* (2000). In this analysis of indentation and perforation process of ductile metal sheets, it was observed that tool load and displacement at perforation initiation, number of petals generated, sheet and petals bending angles, pre and post

† Engineer
‡ Doctor

perforation work inputs and fracture toughness etc. all depend upon the cone angle of indenting conical tool. This dependence is nonlinear giving an optimum value of tool semi angle $\alpha = 35^o$ for easiest perforation. Around this angle, the aluminium sheets showed minimum fracture toughness as well as minimum work input to overcome the offered resistance. This response of parameters versus indenting conical tool semi angle α and especially its optimum behaviour, however, was not adequately and explicit elaborated in previous works. In the present work, this response of various parameters versus conical tool semi angle α is plotted and discussed explicitly with the conclusion that tool angle has an optimum value. This optimal trend of various parameters to the indenting conical tool semi angle is the characteristic of conical tool and has not been observed in sharp tool (Khan 1996, Khan *et al.* 1993, Nazeer *et al.* 1995, Khan and Atkins 1998, Weirzbicki, and Jones 1989) and ball (Khan *et al.* 1995, Khan 1996, Atkins *et al.* 1998) indentation.
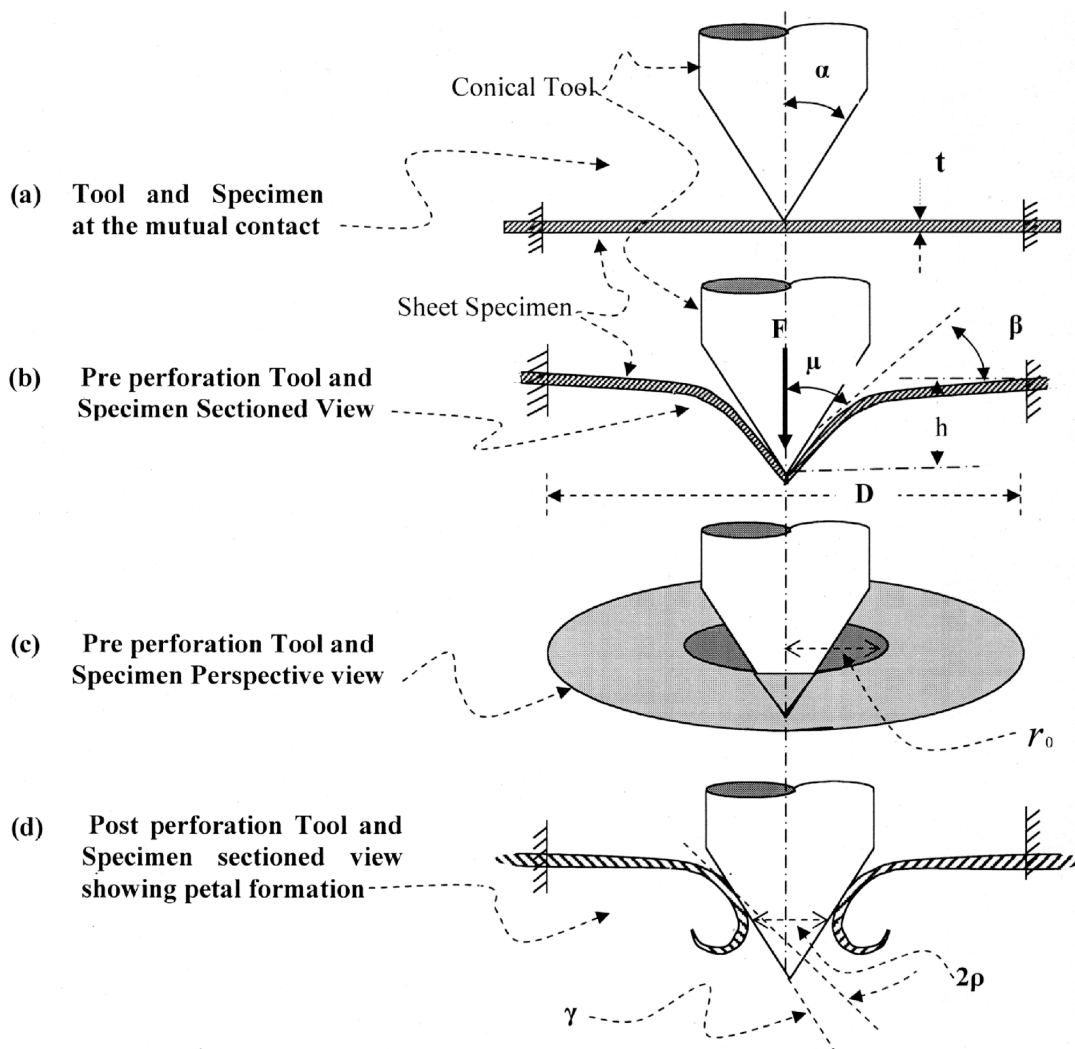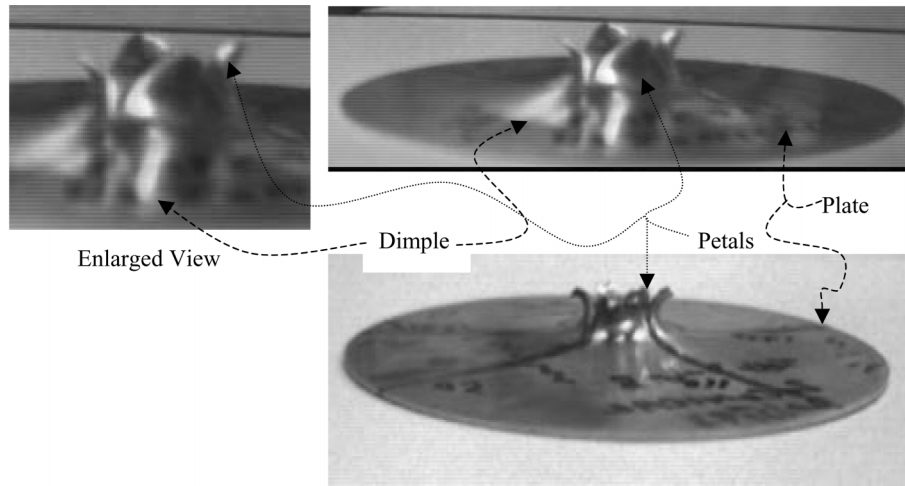

Fig. 1

Fig. 2 Indented sample plates having 4 & 5 petals

As far as, the mechanism leading to the optimum behaviour phenomenon is concerned, Liebowitz (1973), Atkins and Mai (1988), Timoshenko (1986), Giessen *et al.* (1999), Knauss (1993), Timoshenko and Goodier (1951), Horne (1979), Johnson and Mellor (1983) and Johnson *et al.* (1973) have been concerted, but no direct reference to the subject and hence not any direct reference to its mechanics has been found. Liebowitz (1973) discussed various parameters, but in different context and theory elaborated does not match the process in question and also does not explain its optimum behaviour. An ideology explaining the process in question and particularly its optimum behaviour is presented at the end.

2. Experiment

Fig. 1 schematically shows the conical tool indentation with a few parameters. The indentation tests were carried out with the help of the Instron Universal testing machine using 10°, 22.5^o, 35°, 45°, 50° and 60° semi angles conical tools with 6×10^{-6} m/sec indenting speed. For these experiments, 90 mm diameter sheet specimens were cut from SIC half-hard and NS4 aluminum alloy sheets of various thicknesses using manual screw press. The percentage composition of the material by weight with balance aluminium for SIC (approx. AA1100) samples was Fe, Si, Mg, Mn, Zn and Cu as 0.2, 0.3, 0.1, 0.1, 0.1 and 0.1, while that of NS4 (approx. AA5052) was Fe, Si, Mg, Mn, Zn and Cu as 0.5, 0.5, 1.7-2.4, 0.5, 0.25 and 0.25 respectively. As shown in Table 1 below, the tests with all the tools were carried out on SIC half hard 0.66 mm thick sheets, while only three tools with semi angle $\alpha = 10^o$, 35° and 60° were used for sheets of 0.9, 1.2 and 1.5 mm thickness of SIC and 0.56, 0.9 and 1.2 mm thickness for NS4 materials just for results verification. The corresponding load versus displacement data was plotted with x, y chart recorder and diagram were merging together for comparison and relative study. The load versus displacement curves of all the tools for 0.66 mm thick sheet of SIC material presented by Nazeer *et al.* (2000) and Nazeer* *et al.* (2000) is reproduced in Fig. 3 for reference in the discussion. Most of the results presented here in this work are by direct measurements, observations or simple computations, however, computer

program developed on basis of analysis presented by Nazeer *et al.* (2000) was used to get the results of fracture toughness and computed number of petals along with work input distribution estimation for various sharing parameters in both pre and post perforation phases.
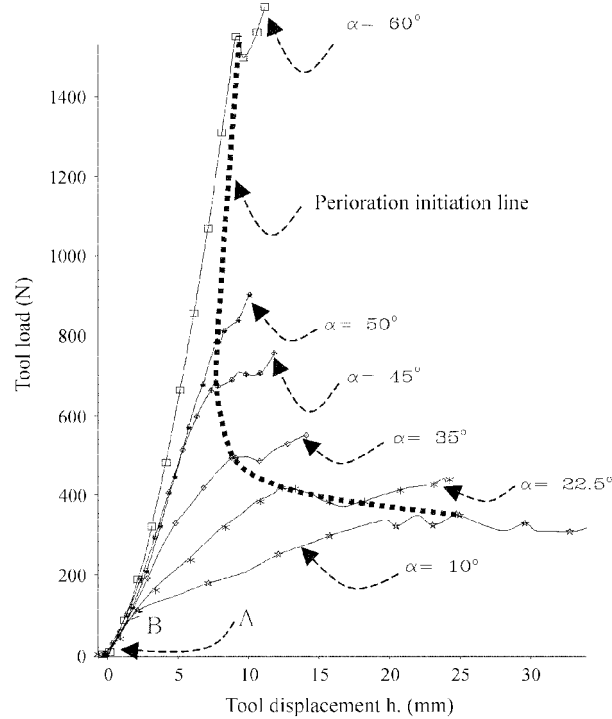

Fig. 3 Tool load versus its displacement for 0.66 mm SIC half hard aluminium sheet (Reprinted by permission of ASM International)

3. Tool angle response analysis

The indentation tests results of various parameters versus conical tool semi angle are plotted in Figs. 4-12 and analyzed in the following paragraphs.

Table 1 Experimental combination of materials, sheets thickness and tools of semi cone angles α

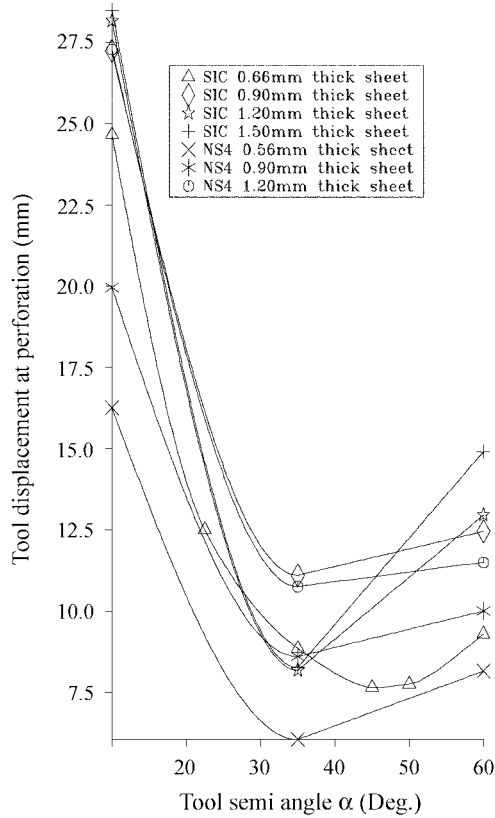| Materiel	Sheet Thickness (mm)	Experiment carried with Conical tool of semi angles α					
		10°	22.5°	35°	45°	50°	60°
SIC Half hard Aluminium alloy (AA 1100)	0.66	√	√	√	√	√	√
	0.9	√	-	√	-	-	√
	1.20	√	-	√	-	-	√
	1.50	√	-	√	-	-	√
NS4 Aluminum alloy (AA 5052)	0.56	√	-	√	-	-	√
	0.9	√	-	√	-	-	√
	1.20	√	-	√	-	-	√

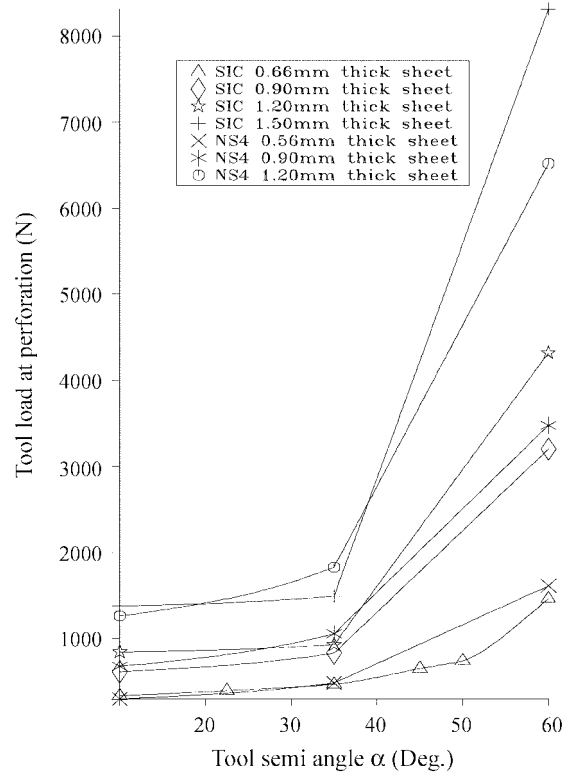Fig. 4 Tool displacement at perforation versus tool semi angle α

Fig. 5 Perforation point load versus tool semi angle α

3.1 Tool displacement at perforation

Tools displacement at the perforation initiation point (h_t) for various sheet thicknesses of both the materials is plotted in Fig. 4 to show their overall trend and mutual comparison. The non-linear trend of all these curves and their turning around $\alpha = 35°$ shows that tool with this cone semi angle is more suitable. The pattern of the curves for various sheet thicknesses of SIC half-hard and NS4 materials show the versatility of above observations with the sheet thickness and also with the sheet material. Curves of SIC half hard aluminium are sharper around $\alpha = 35°$ and it increases with the sheet thickness. It means that SIC half hard aluminium and its sheet thickness is more responsive to the tool angle optimum value $\alpha = 35°$ than NS4.

3.2 Perforation load

Fig. 5 shows the load at the perforation initiation point (F_t) versus tool semi angle α. There is not much difference in load required for perforation initiation up to angle $\alpha = 35°$ but afterwards it increases sharply. From this figure, it is obvious that for all the curves of both materials, $\alpha = 35°$ is the most suitable tool semi angle. Beyond $\alpha = 35°$, the slope of the curves increases with sheet thickness.

3.3 Dimple size

The dimple size has also optimal response with the conical tool semi angle α. The optimal response of its first parameter, the dimple depth given by h_t, the tool pre perforation displacement is elaborated in section 3.1. The optimal response of its second parameter, the radius of the dimple r_0 is shown in Fig. 6. The overall optimal response of dimple deformations in the form of energy input is given in next section.

3.4 Pre-perforation work input

Fig. 7 shows work input prior to perforation initiation points versus tool semi angle α, which is calculated by:

$$W_B = \int_{ho}^{h_t} F dh_i$$

The work input is nonlinear with minimum value at $\alpha = 35°$ for all the samples of both materials. The curves drawn in this Figure also show increase of work input with the thickness of the specimen and that too is tool angle dependent, being minimum at $\alpha = 35°$ with SIC half hard being more responsive to the tool angle variations than NS4.
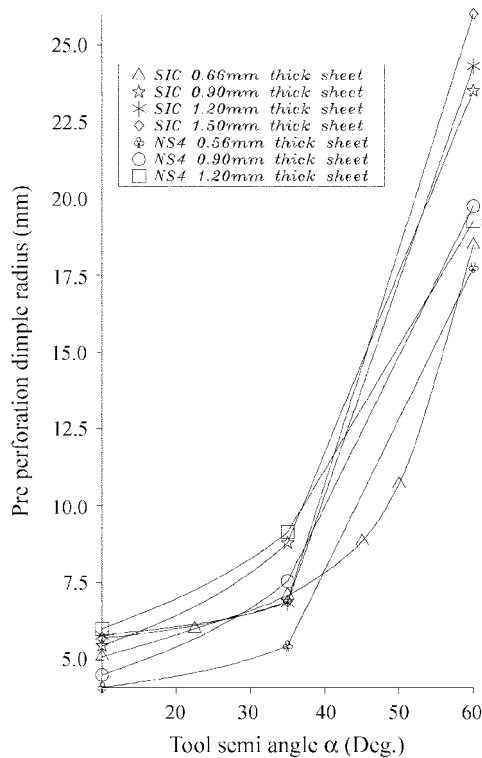

Fig. 6 Pre perforation dimple radius versus tool semi angle α
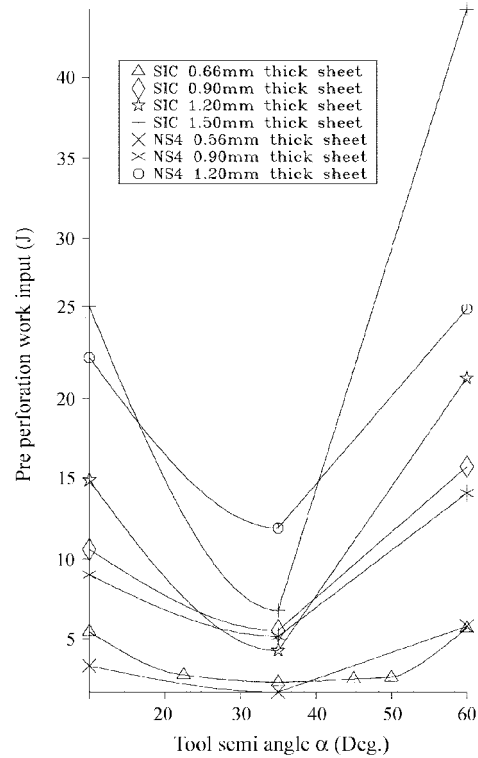
Fig. 7 Pre perforation work input versus tool semi angle α

3.5 Post perforation work input

The post-perforation work input is given by:

$$W_F = \int_{h_t}^{h_i} F dh_i$$

This parameter is not possible to be compared directly, as the further tool displacement is arbitrary, however, post perforation work per unit tool displacement as well as per unit radius of the hole generated can be compared as will be discussed in the following paragraphs.

3.5.1 Post perforation work per unit tool penetration

Fig. 8 shows nonlinearity of work input per unit tool penetration after the perforation initiation versus conical tool angle, giving $\alpha = 35^\circ$ as the most suitable angle and it is also true for other sheet thicknesses of SIC and NS4 materials. The slope of the curves increases with the sheet thickness, showing that $\alpha = 35^\circ$ is the best from this aspect too. Same thicknesses of the two sheet materials have similar behaviour.
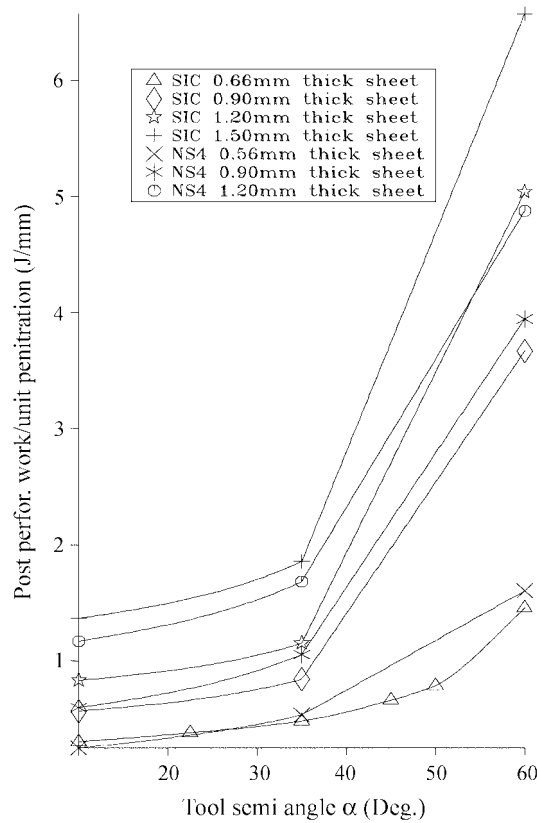

Fig. 8 Post perforation work input per unit tool penetration versus tool semi angle α

3.5.2 Post perforation work per unit hole radius

Fig. 9 shows the work input per unit hole radius versus radius of the hole developed. This shows nonlinearity of work input per unit hole radius development after perforation initiation versus conical tool semi angle. The rate of work input increases with the tool angle deviation from $\alpha = 35^\circ$. The above findings of increase in work input rate with the tool semi angle deviation from $\alpha = 35^\circ$ is more prominent with the increase in the sheet thickness and it shows that tool with angle $\alpha = 35^\circ$ to 50° are most suitable for hole enlargement. The phenomenon of optimal response becomes more prominent as the thickness of the sheet increases, i.e. sharpness of the curve increases with the thickness of the sheet. This behaviour is again non-linear and has an exponential increase with the sheet thickness.

3.6 Fracture toughness

The fracture toughness R versus tool semi angle α for both SIC half hard and NS4 aluminum sheet are evaluated using the analysis and computer code developed by Nazeer *et al.* (1997) and the
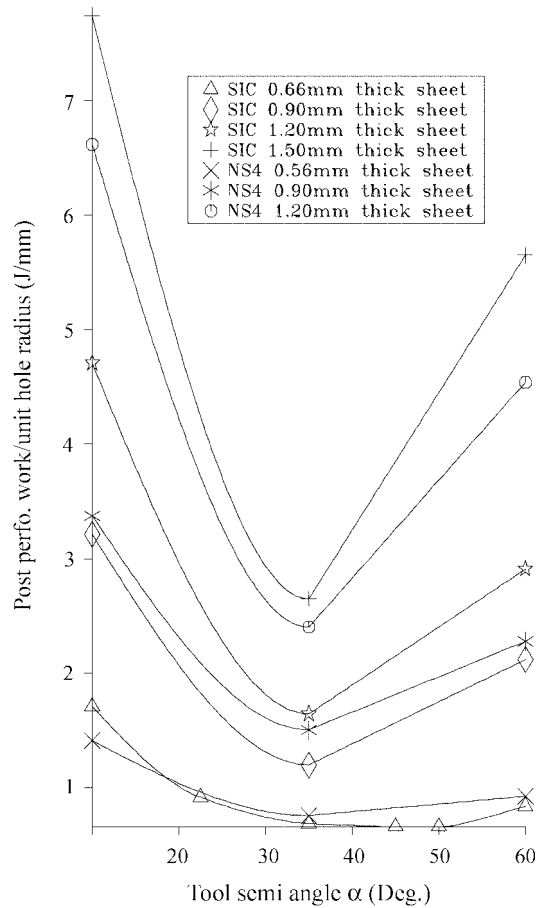

Fig. 9 Post perforation work input per unit hole radius versus tool semi angle α

results presented in Nazeer *et al.* (2000). The resulting curves showed the material and sheet thickness response to the tool angle variation along with their mutual comparison. The dependence of fracture toughness on the tool angle was obvious from all the curves showing optimum tool angle of $\alpha = 35^o$. The minute increase of fracture toughness with the sheet thickness was also clear for both SIC and NS4 sheets except a few departures due to experimental rounding of the actual numbers of petals. This confirmed that tool with $\alpha = 35^o$ was the best and optimum one, requiring minimum work input for crack initiation and tool penetration.

3.7 Sheet bending angle β

Fig. 10 shows the linear trend of sheet bending angle β with slight change in slope at $\alpha = 35^o$ showing its inverse proportionality with the tool semi angle α with minute change in its trend at $\alpha = 35^o$.

3.8 Petals bending angle γ

The mathematical relation (Nazeer *et al.* 2000) which is given by:
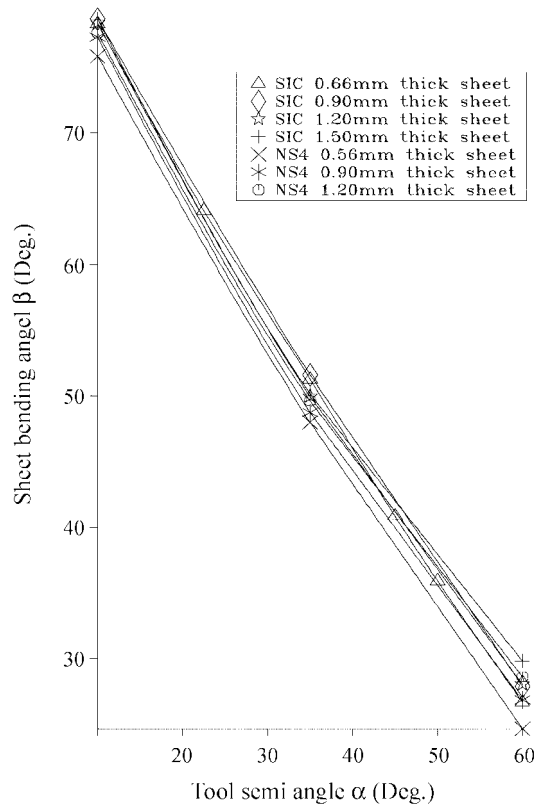
$$\gamma = 90 - \beta - \alpha$$

Fig. 10 Sheet bending angle β versus tool semi angle α

shows the petals bending angle γ dependence on the tool angle. However, Fig. 11 shows its non-linear trend with its optimal dependence on the tool angle having most suitable optimum value of γ at $\alpha = 35°$. Here another aspect is worth noting. Unlike various other parameters, here the behaviour is not systematic with respect to sheet thickness as is obvious in case of SIC half hard material samples. This departure from the normal expected behaviour is due to physically rounding of number of radial cracks and hence the unsystematic sharing or transfer of energy from fracture to petal bending and their strain hardening.

3.9 Computed number of petals

Fig. 12 shows the linear trend of computed number of petals N_c before and after $\alpha = 35°$ with change in trend at this value of tool semi angle, showing its dependence on the tool angle. The slope of curves before the turning value $\alpha = 35°$ is generally less than that after this tool angle. The shown trend of the curves is dependent on the thickness of the sheet. The slop of the curves for thin sheets is larger for small angles than that for larger angles, while it is contrary for the thick sheets.
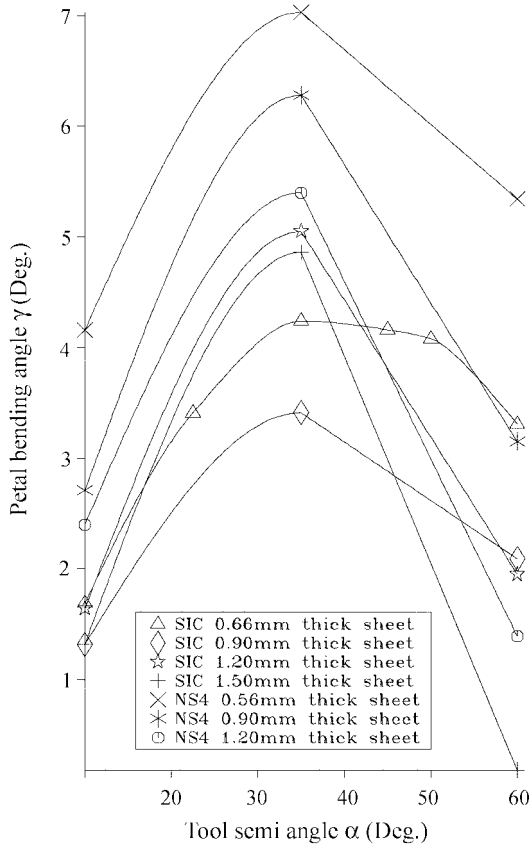

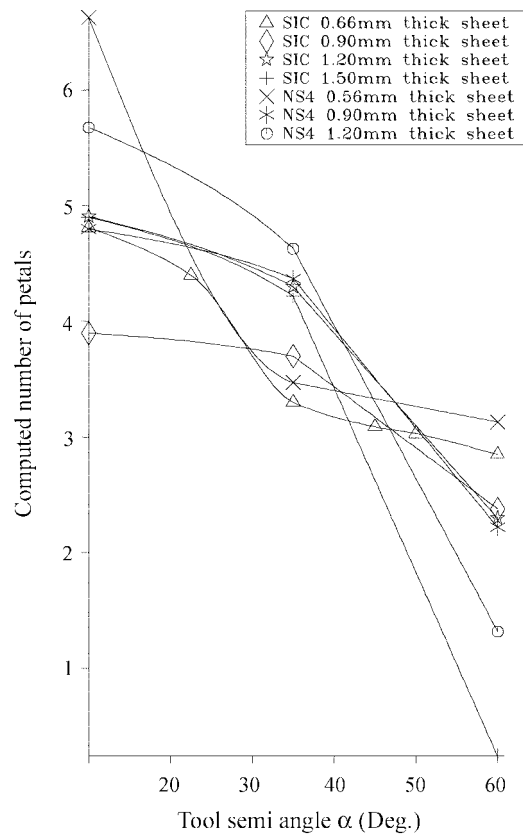Fig. 11 Petal bending angle γ versus tool semi angle α

Fig. 12 Computed number of petals versus tool semi angle α

4. Further deductions

In the pre-perforation phase, the optimal response of W_B and r_o and knowing from Nazeer *et al.* (2000) that:

$$W_B = W_b + W_s$$

it may be concluded that pre perforation stretching work W_s and bending work W_b, also have optimal response with respect to the conical tool semi angle. In the post perforation phase, the work input W_F, (both per unit hole radius and per unit tool penetration) has optimal response with respect to tool semi angle. Knowing its relation with circumferential and radial bending work along with fracture work given by the expression (Nazeer *et al.* 2000):

$$W_F = W_{afc} + W_{afr} + W_f$$

also knowing that the angle γ and the radius of the hole ρ being the main variables in both the post perforation bending works (W_{afc}, W_{afr}), it means that these also have optimal response with respect to the conical tool semi angle α. Similarly the post perforation fracture works W_f also have optimal response with the conical tool semi angle, as its main variables R and N_c are optimally tool semi angle dependent.

5. Mechanics governing the optimal response

Conical tool tip housing (Fig. 1b & Fig. 13a) in the sheet after their mutual contact in place of point contact is the basic governing parameter for the characteristic differences of the corresponding tool angle behaviour. Uptill completion of this housing, the response of all the tools is almost similar (point A to B Fig. 3, O to A being pre housing phase). The diameter of this housing and its depth in the sheet naturally depend upon the tool cone angle. The load is transferred to the specimen through circular cross section around this housing. The sheet is bent and stretched in both radial and circumferential or hoop direction under this load to form cusp or dimple around the housing (Fig. 13a). This process is carried on with minute plastic deformations till μ, the dimple cone semi angle is about 35°. At this point the plastic flow initiates and supercedes most of the working processes. Thus there are two zones of the indenting process, one pre plastic flow perforation process zone with the tool semi cone angle greater than 35° and the other post plastic flow perforation process zone with the tool semi angle smaller than 35°. The two zones are discussed below to highlight the tool angle optimum behaviour.

5.1 Pre plastic flow perforation process zone

Under the tool tip housing loading, the sheet is bent and stretched in both radial and circumferential or hoop direction to form cusp or dimple around the housing (Fig. 13a). This process is carried on with minute plastic deformations till μ, the dimple cone semi angle is about 35°. However this thinning of dimple cone is suppressed and stopped prior to its reaching 35°, if the indenting tools is of cone semi angle larger than 35°. In this case, the tool tightly fits into the
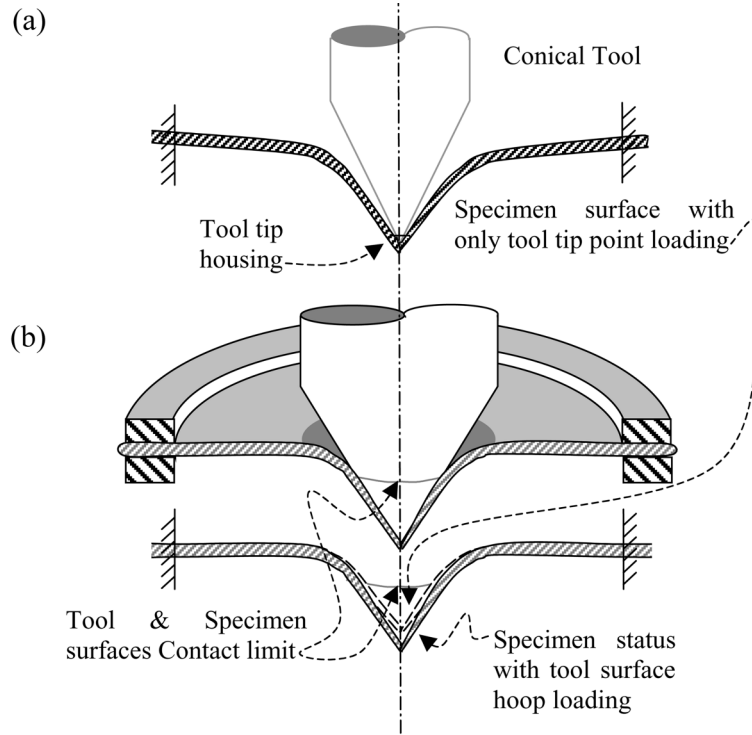
Fig. 13 (a) Pre-perforation tool and specimen view showing tool tip housing loading and elastic - plastic bending and plastic flow stretching, (b) Pre-perforation tool and specimen view showing tool tip surface hoop stress loading and elastic - plastic bending and stretching or plastic flow restraining the inward flow of material below the tool & specimen surfaces contact line

dimple and pushes it along the tool direction of motion without letting the further thinning of dimple cone and this process is carried on till the perforation initiates. The co-linearity of load lines with the tool tip housing process lines (A to B in Fig. 3) clearly indicate the systematic process growth for tool with α = 45, 50 & 60°. This process zone may be named as pre plastic flow perforation process zone. As both the bending force arm and load per unit width or the area at its application point decreases with the increase in cone semi angle, naturally the applied bending moment decreases and hence its effective role decrease too. Thus in this zone, effectiveness of the tool increases with the decrease in tool semi angle.

5.2 Post plastic flow perforation process zone

If the tool cone semi angle is equal to or smaller than 35°, then dimple cone thinning process enters into the plastic flow zone nearly at about μ = 35°. This change in the nature of process is evident in the clear sharp bend in load lines of tool with α = 35, 22.5 & 10°. This cone thinning process may be carried on to wire drawing, but the tools with larger cone semi angle suppress and stop this further thinning of dimple cone and tightly fit into the dimple beyond the initial tool tip housing, pushing it along the tool direction of motion and this process is carried on till the

perforation. During this perforation zone, the earliest stoppage of dimple further thinning has minimum energy input as the further dimple thinning labour is saved. Thus dimple thinning stoppage as early as possible is the best choice and it leads to the largest tool cone semi angle within 35°.

Thus both pre and post plastic flow perforation processes lead to their mutual juncture for optimum response.

5.3 Perforation mechanics

Fig. 14 shows the final schematic of the perforation mechanics in both above stated zones. The bending moment or the bending stress is minimum at the centre of the specimen under the tool tip housing and increases towards the periphery, while radial tensile or stretching stress increases from minimum at periphery to maximum at the centre as shown in Fig. 14. This radial tensile stress gives rise to compressive hoop stress under poisons ratio principle. This results into material flow towards the centre with thinning of the dimple, may it be pre or post plastic flow zone as per analogy presented by Liebowitz (1973). This process carries on till the dimple cone pulls over and tightly grips the tool cone. Here the free compressive hoop stress is forced to change into the tensile hoop stress and the unidirectional inward flow of the specimen material is now restrained up to the tool-specimen contact surfaces limiting line (Fig. 14). Beyond this contact limiting line up to the tool tip, the specimen material flow is radialy outward contrary to the assumption of Liebowitz (1973). Here this tensile hoop stress is most critical, as it is composed of two very critical components given by:

$$T_{th} = T_{ch} + T_{eh}.$$

Here T_{th} is total tensile hoop stress, T_{ch} is component balancing the poisonous compression stress due to radial tensile stress and T_{eh} is the tensile stress component causing the natural circumference (without the tool-specimen surface contact) to increase under their contact. T_{ch} increases exponentially and T_{eh} linearly toward the centre and hence, T_{th} is the most critical, specially at the centre of the specimen. The specimen hence fails under this stress giving rise to number of radial fractures and a few of them may die down prematurely (see Fig. 2) with the subsequent reduction of T_{th} towards the periphery.

The hoop stress beyond the tool-specimen contact surface is again free to result into compression strain, but within the contact limiting line hoop stretching is enforced by the tool contact surface along with radial stretching under poison effect. The friction between the two surfaces in contact is found to be negligible and results with and without lubricant application are almost similar contrary to the assumption of Liebowitz (1973). Fig. 14 illustrates the direction of hoop stress and material plastic flow within and outside the tool-specimen contact surfaces limiting line. As shown in Fig. 14, this partition between the compressive and tensile hoop stresses and reversal of material flow by the contact surfaces limiting line moves towards the periphery of the dimple with the increase in tool angle. This means that point "*L*" (Fig. 14) moves away from O with increase in the tool semi cone angle.
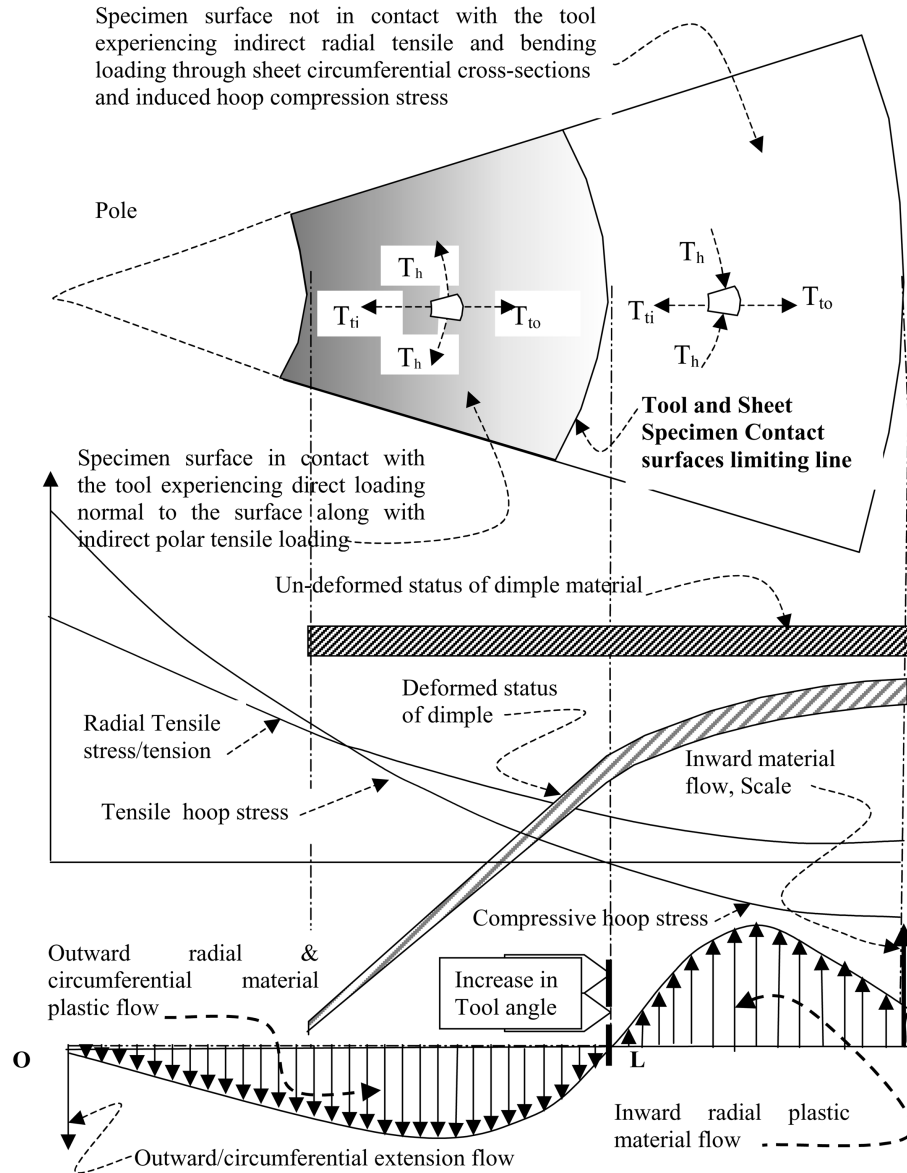
Specimen surface not in contact with the tool experiencing indirect radial tensile and bending loading through sheet circumferential cross-sections and induced hoop compression stress

Pole

T_h

T_{ti} T_{to}

T_h

T_h

T_{ti} T_{to}

T_h

Tool and Sheet Specimen Contact surfaces limiting line

Specimen surface in contact with the tool experiencing direct loading normal to the surface along with indirect polar tensile loading

Un-deformed status of dimple material

Deformed status of dimple

Inward material flow, Scale

Radial Tensile stress/tension

Tensile hoop stress

Compressive hoop stress

Outward radial & circumferential material plastic flow

Increase in Tool angle

O   L

Inward radial plastic material flow

Outward/circumferential extension flow

Fig. 14 Hoop and meridian stresses within dimple and their variation with the tool angle

6. Conclusions

From the above discussions it has been concluded that

1. The $\alpha = 35°$ is the most suitable and optimum value for the tool semi angle α in all respects for these sheet metals indentation and perforation with conical tool.
2. The ductile metal sheet offer minimum resistance to the conical tool of semi angle $\alpha = 35°$.

3. R, W_B, W_b, W_s, W_F, W_f, W_{af}, W_{afc}, W_{afr}, β, γ, h_t and r_o all have optimum response with respect to conical tool semi angle.

4. The results were reproduce-able in the ductile metals.

5. The fracture with conical tool has two modes, the pre plastic flow perforation process mode zone and the post plastic flow perforation process mode zone. Both these modes leading the process to an optimum value at their mutual juncture at $\alpha = 35^\circ$.

6. Specimen material failure is solely under the tensile hoop stress and hence results into radial cracks initiation and propagation.

References

Atkins, A.G. and Mai, Y.W. (1988), *Elastic and Plastic Fracture*, John Wiley, Chechester, UK.

Atkins, A.G., Khan, M.A. and Liu, J.M. (1998), "Necking and radial cracking around perforation in the sheet of normal incidence", *Int. J. Impact Eng.*, **21**(7), 521-539.

Giessen, E.V.D., Estevez, R., Pijnenburg, K.G.W. and Tijssens, M.G.A. (1999), "Computational modeling of failure process in polymers", *Proc. of ECCM99 European Conf. Comput. Mech.*, Aug. Sept.

Horne, M.R. (1979), *Plastic Theory of Structures*, Pergamon press.

Johnson, W., Chatkara, N.R., Ibrahim, A.H. and Dasgupta, A.K. (1973), "Hole flanging and punching of circular plates with conically headed cylindrical punch", *J. Strain Analysis*, **8**, 228-242.

Johnson, W. and Mellor, P.B. (1983), *Engineering Plasticity*, edited by Atkins A.G., Ellis Harwood, Chechester, UK.

Khan, M.A., Nazeer, M.M., Naeem, A., Haq, A-ul and Atkins, A.G. (1995), "Computer modeling of elasto-plastic fracture mechanics of ball indentation in ductile aluminum sheet", *Proceedings of '95 EUROMAT, European Conference on Advanced Materials and Processes, Symposium D,* Padua/Venice Italy, September.

Khan, M.A. (1996), "Indentation and perforation in ductile metal sheets", *Ph. D. Thesis,* Reading University, Reading, UK.

Khan, M.A., Naeem, A., Nazeer, M.M., Haq, A-ul and Atkins, A.G. (1993), "Analysis of curvature generation and fracture toughness of indented aluminium sheet", *Proc. ISAM 1993, 3rd Int. Symp. on Advanced Materials,* Islamabad, Pakistan, September.

Khan, M.A. and Atkins, A.G. (1998), "Cutting of ductile metal sheet by asymmetric pointed tools", *Journal of Material Processing Technology,* **82**, 172-178.

Knauss, W.G. (1993), "Time dependent fracture and cohesive zones", *J. Eng. Mat. Tech.*, **115**, 262-267.

Liebowitz, H. (1973), *Fracture an Advanced Treatise*, Vol.1-12, Academic press N Y, San Francesco, London.

Nazeer, M.M., Khan, M.A., Naeem, A., Haq, A-ul and Atkins, A.G. (1995), "Mathematical analysis of indented aluminium sheet curvature", *Proc. ICPAM 95 Int. Conference on Pure and Applied Mathematics,* Bahrain.

Nazeer, M.M., Naeem, A., Khan, M.A., Haq, A-ul and Atkins, A.G. (1997), "Metal sheet behavior in conical tool indentation", *Proceedings ISAM 1997, 5th Int. Symposium on Advanced Materials,* Islamabad, Pakistan, September.

Nazeer, M.M., Khan, M.A., Naeem, A. and Haq, A-ul. (2000), "Mathematical analysis of ductile metal sheets indentation with conical tool", *Int. J. Mechanical Science*, **42**(7), 1391-1403.

Nazeer*, M.M., Khan, M.A., Naeem, A. and Haq, A-ul. (2000), "Response of ductile metal sheet parameters to the cone angle of an indenting conical tool", *Int. J. Material Engineering and Performance*, **9**(5), 478-489.

Timoshenko, S. (1986), *Strength of Materials, Part 2, Advanced Theory and Problems*, 3rd edition, CBS Publishers & Distributors, Delhi, India.

Timoshenko, S. and Goodier, J.N. (1951), *Theory of Plasticity*, McGraw-Hill, N. Y.

Weirzbicki, T. and Jones, N. (1989), *Structure Failure*, edited by Atkins, A.G., John Wiley & Sons, Inc.

Notation

F	Applied force
F_t	Perforation point tool load
h_0	Tool displacement at its contact with the sheet specimen
h_t	Tool displacement at perforation initiation
h_i	Instantaneous Tool displacement
W_B	Pre perforation work input
W_b	Pre perforation bending work input
W_s	Pre perforation stretching work input
W_F	Post perforation work input
W_{af}	Post perforation bending work input
W_{afc}	Post perforation circumferential bending work input
W_{afr}	Post perforation radial bending work input
W_f	Post perforation fracture work input
N_c	Computed Number of petals
ρ	Perforated hole radius
r_o	Dimple radius
R	Fracture toughness
α	Conical tool semi angle
μ	Dimple Cone semi angle prior to perforation
β	Sheet bending angle
γ	Petal bending angle